

Glass beads increase the formation kinetics of beta-lactoglobulin amyloid fibrils

Food Hydrocolloids

Heyn, Timon R.; Schrader, Marcel; Kampen, Ingo; Kwade, Arno; Schwarz, Karin et al https://doi.org/10.1016/j.foodhyd.2023.108511

This publication is made publicly available in the institutional repository of Wageningen University and Research, under the terms of article 25fa of the Dutch Copyright Act, also known as the Amendment Tayerne.

Article 25fa states that the author of a short scientific work funded either wholly or partially by Dutch public funds is entitled to make that work publicly available for no consideration following a reasonable period of time after the work was first published, provided that clear reference is made to the source of the first publication of the work.

This publication is distributed using the principles as determined in the Association of Universities in the Netherlands (VSNU) 'Article 25fa implementation' project. According to these principles research outputs of researchers employed by Dutch Universities that comply with the legal requirements of Article 25fa of the Dutch Copyright Act are distributed online and free of cost or other barriers in institutional repositories. Research outputs are distributed six months after their first online publication in the original published version and with proper attribution to the source of the original publication.

You are permitted to download and use the publication for personal purposes. All rights remain with the author(s) and / or copyright owner(s) of this work. Any use of the publication or parts of it other than authorised under article 25fa of the Dutch Copyright act is prohibited. Wageningen University & Research and the author(s) of this publication shall not be held responsible or liable for any damages resulting from your (re)use of this publication.

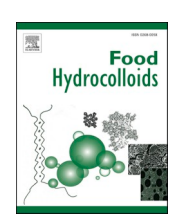
For questions regarding the public availability of this publication please contact $\frac{openaccess.library@wur.nl}{openaccess.library@wur.nl}$

ELSEVIER

Contents lists available at ScienceDirect

Food Hydrocolloids

journal homepage: www.elsevier.com/locate/foodhyd





Glass beads increase the formation kinetics of beta-lactoglobulin amyloid fibrils

Timon R. Heyn^a, Marcel Schrader^b, Ingo Kampen^b, Arno Kwade^b, Karin Schwarz^{a,*}, Julia K. Keppler^c

- ^a Institute of Human Nutrition and Food Science, Division of Food Technology, Kiel University, 24118, Kiel, Germany
- ^b Institute for Particle Technology, Technische Universität Braunschweig, 38104, Braunschweig, Germany
- c Laboratory of Food Process Engineering, Wageningen University, Bornse Weilanden 9, 6708WG, Wageningen, P.O. Box 17, 6700 AA, Wageningen, the Netherlands

ARTICLE INFO

Keywords: Whey-protein Beta-lactoglobulin Fibrils Amyloid aggregates Orbital agitation Beads

ABSTRACT

In this study beta-lactoglobulin solutions were processed with glass beads in an orbital shaker at high temperatures and low pH value to identify the effect of mechanical stressing and surfaces on amyloid aggregation kinetics. The information will provide a better understanding on how specific mechanical factors provide a nucleation supporting effect on the assembling of building blocks for a more efficient production of functional amyloid aggregates. Because aggregate morphologies vary at pH 2 (semiflexible) or pH 3.5 (worm-like), examination at both pH values gives information about their specific formation and stability characteristics. Different diameters of glass beads (20–1000 µm), and different shaking frequencies (0 - 280 min⁻¹) were used to vary mechanical stress energy, which was quantified by CFD-DEM simulations. To investigate surface effects, the hydrophobicity and surface roughness of glass beads was altered by modification with stearic acid. Amyloid aggregates and bead surfaces were analysed by ThT-assay, AFM and ATR-FTIR.

Hydrophobic beads with high surface roughness affected the aggregation negatively. The use of non-hydrophobic beads increased the formation kinetics of fibrils but not of worm-like aggregates, although, both morphologies had a reduced mean length.

1. Introduction

There is an increasing interest in exploring amyloid fibrils for their functional properties in foods with regard to gelling (Gosal et al., 2004; Kavanagh et al., 2000a; Mudgal, Daubert, & Foegeding, 2011), emulsification (Gao et al., 2017; Mantovani et al., 2017; Serfert et al., 2014), and foaming (Oboroceanu et al., 2014; Peng et al., 2017). Further, the use of engineered fibrils as nanocomposites and hybrid materials for biosensors and medical applications (Bolisetty et al., 2014; Li et al., 2012, 2013; Sasso et al., 2014), photovoltaics (Bolisetty et al., 2012), catalytic purposes (Bolisetty et al., 2015) or for water purification (Bolisetty et al., 2015) is currently being explored. However, the procurement of fibrils as a starting material for all these applications has so far required a great expenditure of energy and production time.

Beta-lactoglobulin (BLG), the main protein in the whey fraction of bovine milk, is one of the most studied food proteins in terms of amyloid formation and gives therefore an excellent basis for further and deeper investigations. High temperatures (>80 $^{\circ}\text{C})$ and low pH values are required to form amyloid fibrils (i.e., stacked beta sheet formations with a high aspect ratio) from BLG (Cao & Mezzenga, 2019; Loveday et al., 2017). Depending on the process parameters, different amyloid (like) morphologies occur, for example straight fibrils of hydrolysed peptides at pH 2 or worm-like aggregates of intact BLG at pH 3.5 (Heyn et al., 2019; vandenAkker et al., 2016; Ye et al., 2018). The use of chemicals, enzymes, solvents and microwave radiation to produce amyloid aggregates at lower temperatures was also tested but led to structural deviation (Hoppenreijs et al., 2022) or risk of toxicity of the end product (Cao & Mezzenga, 2019). In contrast, stirring and shearing seem to reduce the required production time of fibrils at > 80 °C from \sim 24 h to only 5 h without undesired effects (Akkermans et al., 2006; Bolder et al., 2007; Dunstan et al., 2009; Ng et al., 2016). Energy intake by agitation of the protein solution was described earlier to enhance (amyloid) aggregation for different kinds of proteins (Ladner-Keay et al., 2014; Macchi et al., 2011; Sluzky et al., 1991). The addition of 1-1.5 mm beads into the agitation vessel has led to an increase in the formation kinetics of

E-mail addresses: theyn@foodtech.uni-kiel.de (T.R. Heyn), marcel.schrader@tu-braunschweig.de (M. Schrader), i.kampen@tu-braunschweig.de (I. Kampen), a.kwade@tu-braunschweig.de (A. Kwade), info@foodtech.uni-kiel.de (K. Schwarz), julia.keppler@wur.nl (J.K. Keppler).

^{*} Corresponding author.

BLG

Abbreviations

AFM Atomic Force Microscopy APTES Aminopropyltriethoxysilane

ATR-FTIR Attenuated Total Reflection Fourier Transform

Infrared Spectroscopy Beta-Lactoglobulin

CFD Computational Fluid Dynamics DEM Discrete Element Method DIC N,N-Diisopropylcarbodimid

MS Mass Spectrometry ThT Thioflavin-T

UV/VIS Ultraviolet–Visible Spectroscopy

pathogenic amyloid structures from alpha-synuclein (Pronchik et al., 2010). The higher mechanical stress as well as the effect of the particle surface were described as influencing factors (Grigolato & Arosio, 2021; Macchi et al., 2011; Pronchik et al., 2010). Here, interfaces and shear stress influence different mechanisms in the nucleation process of human pathogenic amyloid structures (Grigolato & Arosio, 2021). It is not yet known whether engineered amyloid fibril formation can also be induced by the presence of beads. If this would be possible such aggregates could be produced more efficiently in the future.

Furthermore, different morphologies and aspect ratios of (amyloid) aggregates affect their functional properties at interfaces, as they occur in emulsions and foams (Hoppenreijs et al., 2022; Serfert et al., 2014). In order to use fibrils as functional additives, it is therefore of interest to be able to produce their shape (e.g. length) in a controlled manner.

In order to investigate the effects of mechanical energy input and particle surface on amyloid aggregation of BLG at pH 2 (fibrils) and pH 3.5 (worm-like aggregates) at the threshold temperature of amyloid aggregation of 70 °C (Heyn et al., 2020), glass beads of different size classes (0–20, 100–200, 400–600 and 750–1000 μm), and thus different particle masses and surface areas were used. To vary the kinetic energy transferred to stressing energy, different particle masses and particle velocities (shaking frequency between 60 and 280 min⁻¹) were used. The mechanical stresses were quantified based on the model of (Kwade, 2003) via the stress energy (SE), the stress frequency (SF) and the power input using CFD-DEM simulations. Here, the SE describes the maximum energy that could be transferred to product particles by normal impact or shearing at the moment of a collision. Furthermore, the product of the frequency of collisions per time unit (SF) and SE gives the power input. The effect of the bead surface (hydrophobicity and roughness) on the amyloid aggregation was examined, by modifying the beads with hydrophobic stearic acid.

These experiments will provide a better understanding on the formation of straight fibrils and wormlike amyloid (-like) aggregates. Additionally, new ways for a faster production of fibrils can be achieved. This may help to reduce process expenses such as time and energy input.

2. Materials and methods

2.1. Materials

Beta-Lactoglobulin (BLG) was obtained from *Davisco Foods International, Inc (Eden Prairie, USA)* with 97% protein and 96% BLG in dry matter. Calculated NaCl content was 0.0496 mmol/g protein. SiLibeads Glass Beads Typ S and SiLibeads Solid Micro Glass Beads of different size classes were kindly made available by *Sigmund Lindner GmbH (Germany)*. The measured mean diameters were \sim 870, \sim 520, \sim 170 and \sim 6.6 µm, respectively (see Table 1). Thioflavin-T (ThT >95%) was obtained from *EMD Millipore Corp. (USA)*. 3-aminopropyltriethoxysilane (APTES \geq 98.0%) and N,N-diisopropylcarbodimid (DIC \geq 99%) were

Table 1

Glass bead characterization. Mean and standard deviation (SD) of the diameter and spec. surface was measured by static light scattering and calculated by the application software. All measurements were conducted in triplicate. The specific surface per gram glass beads was calculated using a material density of 2.5 g/cm^3 . The bound stearic acid was calculated with a surface coverage of $1 \text{ molecule per nm}^2$.

-				
Glass bead type	Typ S 750–1000 μm	Typ S 400–600 μm	Solid 100–200 μm	Solid 0–20 μm
Diameter \pm SD [μ m]	870 ± 110	519 ± 84	171 ± 44	6.6 ± 2.3
Spec. surface [cm ² /g]	28.02	47.47	147.54	4137.65
Surface of 5 g glass beads [cm ²]	140.08	237.37	737.71	20 688.27
Bound stearic acid on 5 g glass beads [nMol]	46.5	78.8	245.0	6870.9
Ratio beta-lactoglobulin: stearic acid	1476.3	871.2	280.3	9.996

obtained from Sigma Aldrich Inc. All other chemicals were of analytical grade and obtained from Sigma Aldrich Inc. The experiments were conducted with ultrapure water (>17 M Ω cm; total oxidizable carbon < 5 ppb).

2.2. Preparation of materials

2.2.1. Preparation of BLG solutions

BLG was predissolved in ultrapure water, adjusted to the desired pH value of 2.0 or 3.5, using 6 M and 1 M HCl and then diluted to a final protein concentration of 2.5 wt% BLG. The pH value was subsequently readjusted.

2.2.2. Preparation of stearic acid modified glass beads

Glass beads were activated for 15 min at room temperature in a 4 M NaOH solution and were modified as described by (Kockmann et al., 2015): Glass beads were boiled in 21,4 mM 3-aminopropyltriethoxysilane (APTES)-ethanol solution for 15 h at 78 °C in a reflux cooling system. After washing 6 times with ethanol, APTES modified glass beads were dried at 80 $^{\circ}$ C. 50 ml of a 33 mM stearic acid-ethanol solution was prepared and agitated with N,N-diisopropylcarbodimid (DIC) at a molar ratio of 1:1.5 for 30 min. Glass beads were added and covalent binding of stearic acid on APTES molecules was induced for >15 h at room temperature under agitation at 150 min⁻¹. Afterwards, glass beads were washed 6 times with ethanol and dried under vacuum (50 mbar) before usage. The glass bead modification was confirmed with attenuated total reflection Fourier-transform infrared spectroscopy (ATR-FTIR) (see 2.4.4 for more details). The concentration of free APTES, DIC and stearic acid after each washing step was checked by using mass spectrometry (MS) (results not shown). The particle size distribution of the glass beads was measured by static light scattering (see 2.4.3 for more details).

2.3. Processing of native BLG and fibril solutions

For investigations of the mechanical stress and influence of the glass bead surface on fibril formation, modified and unmodified glass beads were agitated in a thermo-controlled shaking incubator (KS 4000 ic, IKA-Werke GmbH & CO. KG, Staufen, Germany). Native BLG-solutions with a pH value of 2 or 3.5 were added to the glass beads into 250 ml shaking flasks with four baffles. The flasks were fixed on the agitation plate of the incubator and the temperature was set to 80 °C and monitored by sensors next to the samples. The solution temperature was between 67 °C and 71 °C. The shaking frequency was set to 60, 120, 180 or 280 min $^{-1}$ at an orbital radius of 1 cm. For sampling after 0.5, 1, 2, 3 and 4 h, the shaking was interrupted for 1 min. All experiments were conducted as independent replicates. Agitation at 180 and 280 min $^{-1}$ had the strongest effects on the fibril formation kinetics (see supplementary material

TAB S3 – S5), therefore the investigations were focused on these samples. The concentration of free stearic acid in the solution during the amyloid fibril formation process in the presence of stearic acid modified glass beads was controlled by using MS (results not shown). The sample absorbance was analysed by UV/VIS (ultraviolet–visible) spectroscopy at 278 nm (*Helios-Gamma, ThermoFisher Scientific, Waltham, USA*) to control the protein concentration and the loss of protein via adsorption of BLG to the glass beads.

2.4. Analytical methods

2.4.1. Amyloid formation by Thioflavin-T (ThT) assay

The quantification of the amyloid aggregate formation was investigated by ThT assay as described by (Keppler et al., 2019). 48 μ l of the to 1% diluted sample were mixed with 4 ml phosphate buffered ThT-solution. After 60 s of incubation ThT-fluorescence was measured in a fluorescence spectrophotometer (*Cary Eclipse, Varian GmbH Darmstadt, Germany*) at 440 nm excitation and 482 nm emission wavelength.

2.4.2. Fibril morphology and glass bead surface by atomic force microscopy (AFM)

The fibril morphology was investigated by using AFM (*NanoWizard 3, JPK Instruments AG (today Bruker Nano GmbH), Berlin, Germany*), following the preparation protocol of (Serfert et al., 2014) and (Adamcik et al., 2010). For the tapping mode, a SHR300 probe was used (force constant 40 N/m, resonance frequency 300 kHz; *BudgetSensors, Innovative Solutions Bulgaria Ltd., Sofia, Bulgaria*) at a scan rate of 0.6 Hz. For the investigation of the glass bead surfaces, the beads were attached to an object slide by superglue and measured with a SHR75 probe (force constant 3 N/m, resonance frequency 75 kHz, *BudgetSensors, Innovative Solutions Bulgaria Ltd., Sofia, Bulgaria*) at a scan rate of 0.6 Hz.

The statistical tools of *Gwyddion 2.53* were used for the calculation of the maximum peak high and mean roughness (σ) of the AFM scanned glass bead surfaces ($5 \times 5 \mu m$) from six different glass beads. Statistical values were calculated from height irregularities ($z_n - z$) with z as average high value (equation (1)).

$$\sigma = \frac{1}{N} \sum_{n=1}^{N} (z_n - z) \tag{1}$$

2.4.3. Glass bead characterisation by static light scattering

The particle size distribution of the glass beads was analysed by using static light scattering (refractive index of 1.51, *Horiba LA-950V2, Retsch Technology, today Microtrac Retsch GmbH, Haan, Germany*) at dry mode. The mean and standard deviation (SD) of the diameter and spec. surface were calculated by the application software (*Horiba LA-950 V.7.02, Horiba Jobin Yvon GmbH, Beinsheim, Germany*) (see Table 1). The surface of 5 g glass beads was calculated assuming a material density of 2.5 g/cm³. The bound stearic acid was calculated with a surface coverage of ~1 molecule per nm² (Zarinwall et al., 2021).

2.4.4. Glass bead surfaces by ATR-FT infrared spectroscopy

Infrared spectra of the glass bead surfaces were analysed using a Tensor 2 System from Bruker Optik GmbH, Ettlingen, Germany fitted with a at 25 °C thermally controlled BioATR Cell 2. The $\sim\!6.6~\mu m$ glass beads were placed on the ATR crystal before or after their modification, or after their use in the fibril formation process. The spectra were acquired and averaged over 120 scans at a resolution of 0.7 cm $^{-1}$. After atmospheric correction for absorbance of CO $_2$ and H $_2$ O as vapour, the protein spectra from 4000 cm $^{-1}$ to 900 cm $^{-1}$ were baseline corrected.

2.5. Quantification of the mechanical stress via CFD-DEM simulations

In order to quantify the mechanical stress caused by the addition of glass spheres, computational fluid dynamics (CFD) simulations were carried out in combination with the discrete element method (DEM) to

investigate the three-phase flow. The basic simulation setup, which is based on the open-source software LIGGGHTS (DEM) (Kloss et al., 2012), OpenFOAM (CFD) and CFDEMcoupling (Goniva et al., 2012), was adopted from Schrader et al. (2019). However, the surface tension force was neglected as a coupling force, as its use can lead to unstable simulations in some cases. The particle and wall DEM parameters were adapted and the fluid properties were adjusted according to Table 2. A DEM time-step of $1 \cdot 10^{-6}$ s and a CFD-DEM coupling interval of 10 were used. In total eight simulations were carried out for two particle sizes (870.72 μ m and 519.68 μ m) and four different agitation speeds (60, 120, 180, 280 min $^{-1}$, orbital shaking radius 1 cm).

By the specific evaluation of the bead-bead and bead-wall collisions according to Beinert et al. (2015), coupled CFD-DEM simulations provide quantitative data on the magnitude of the stress energy and frequency for different experimental test parameters. For a deeper understanding of the dominant stress mechanism, the stress energies were subdivided into normal and shear contacts.

2.6. Statistical analysis

Statistical analysis of the collected data was conducted by GraphPad PRISM (*version 9.0.2, GraphPad Software, San Diego, USA*). Significance of the results was tested by 2-way ANOVA with an alpha of 0.05. Multiple comparisons were corrected with the Tukey post hoc test.

3. Results

3.1. Characterisation of glass bead surfaces

The surface chemistry of the smallest particle size (\sim 6.6 μ m) could be investigated by ATR-FTIR. Coarser beads did not provide enough contact area to the surface of the ATR-crystal for a sufficient signal-tonoise ratio. The absorption of wavenumbers in the asymmetric and symmetric stretching area of CH3 and CH2 compounds (2960 - 2800 cm⁻¹) reflects the surface coating with a lipid (here stearic acid). Absorptions at the wavenumbers of the Amide I (1700 - 1600 cm⁻¹) and Amide II (1555 - 1535 cm⁻¹) region revealed the occupation of the surface with proteinogenic compounds. The 2-step modification of the glass bead surface, first with APTES and then with stearic acid, led to an absorption in the CH stretching area (Fig. 1 A). As visible in Fig. 1 B, the adsorption of proteinogenic material to the surfaces of unmodified beads was higher compared to stearic acid modified beads. Furthermore, the Amide I band of stearic acid modified beads incubated in pH 2 and pH 3.5 BLG solution, as well as unmodified beads incubated in pH 3.5 solution, showed a slight "shoulder" at 1620 cm⁻¹.

The analysis of the physical surface properties with the help of AFM gave evidence that by treating the glass surfaces of glass beads with 4 M NaOH, the surface relief was smoothed (FIG 2 A compared to B and C). The calculated mean roughness (deviation from the statistical mean height value) decreased by 90–94%. The modification of the spherical surfaces with stearic acid led to the presence of punctual elevations with a maximum peak height (difference from the average height relief) of $\sim\!48\pm9$ nm (FIG 2 C).

Table 2Fluid properties used for the CFD-DEM simulation.

Fluid parameters		Liquid	Air (interpolated for 69 °C) (Kleiber & Joh, 2013))
Dyn. Viscosity	[mPas]	0.80 (Heyn et al., 2020)	$2.05 \bullet 10^{-2}$
Density	[kg m ⁻³]	1001 (Heyn et al., 2020)	1.02
Surface tension (water)	$[mN \\ m^{-1}]$	64.66 (Vargafti	k et al., 1983)

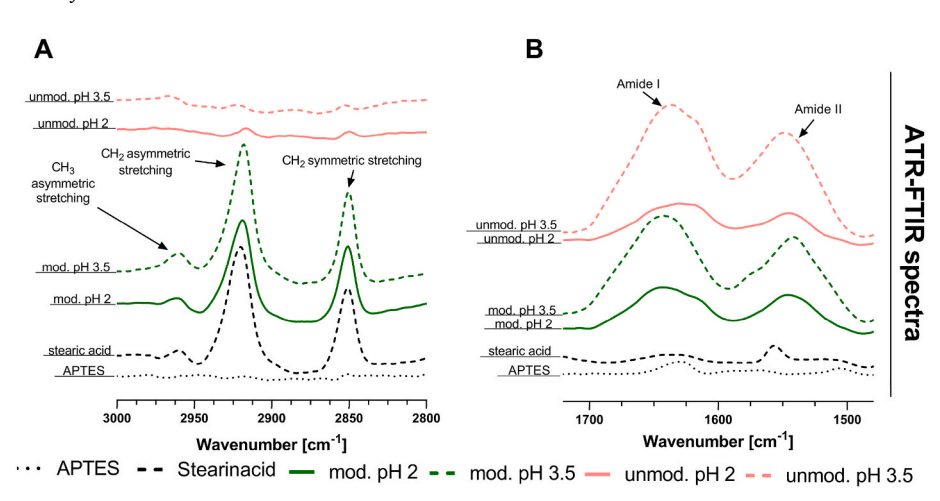


Fig. 1. ATR-FTIR spectra of modified and unmodified \sim 6.6 μm glass beads. Lipid relevant CH₃ asymmetric (2950–2960 cm⁻¹), CH₂ asymmetric (2915–2930 cm⁻¹) and CH₂ symmetric stretch region (2852–2800 cm⁻¹) (A) and protein relevant Amid I (1700–1600 cm⁻¹) and Amid II band (1555–1535 cm⁻¹) (B) of modified and unmodified glass beads. APTES: with 3-Aminopropyltriethoxysilan modified glass beads (after APTES modification). Mod. pH 2/pH 3.5: stearic acid modified glass beads which were agitated at 80 °C in pH 2/pH 3.5 BLG solution. Unmod. pH 2/pH 3.5: unmodified glass beads which were agitated at 80 °C in pH 2/pH 3.5 BLG solution.

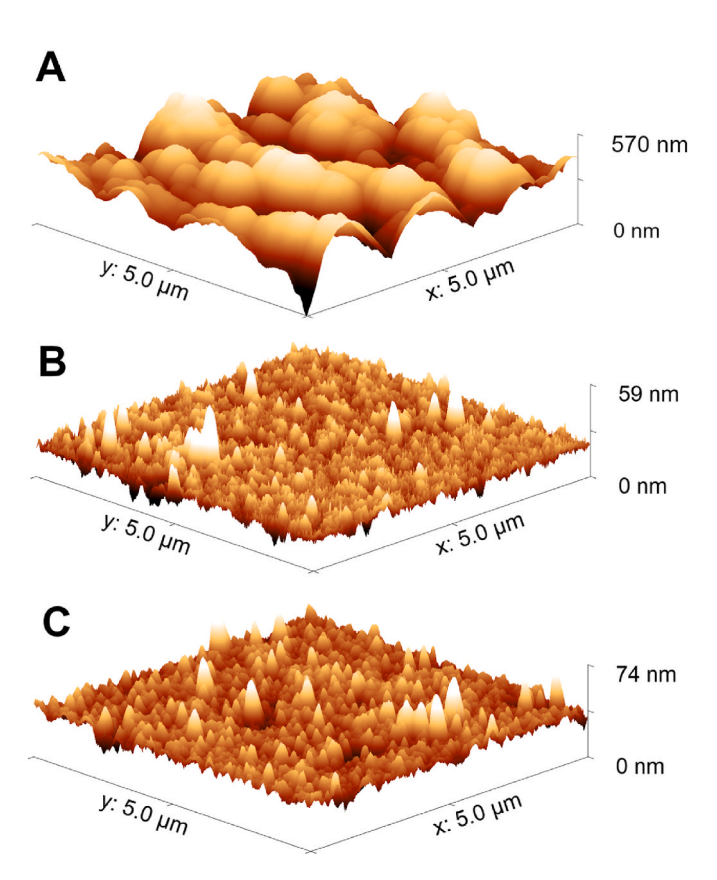


Fig. 2. Atomic Force Microscopy scanned surfaces of unmodified (A), 4 M sodium hydroxide treated (B), or covalently bonded stearic acid modified (C) glass beads with a diameter of ${\sim}520~\mu m$. The z-axis was scaled for better visibility of the relief.

3.2. Influence of particle size and shaking frequency on amyloid aggregation

The use of unmodified glass beads in the agitation incubator at pH 2 and $>70~^\circ\text{C}$ generally produced a greater increase in ThT-fluorescence (ThT-Fl.) over time than agitating without glass beads (Fig. 3 A vs. B - E). By agitating without the glass beads, the ThT-Fl. rose from 5.0 A.U. to 7.1 within 5 h incubation. Increasing the bead size roughly resulted in a minor increase of the ThT-Fl during the 5 h incubation: By using glass beads at 180 min $^{-1}$, a maximum ThT-Fl. of 11.6 A.U. ($\sim\!6.6~\mu\text{m}$ beads), 16.2. A.U. ($\sim\!170~\mu\text{m}$ beads), 13.8 A.U. ($\sim\!520~\mu\text{m}$ beads), and 17.4 A.U. ($\sim\!870~\mu\text{m}$ beads) were reached (Table 3).

The use of small beads (\sim 6.6 µm) in combination with a higher shaking frequency of 280 min⁻¹ increased the maximum ThT-Fl. after 5 h from 5 to 14.0 A.U. (Fig. 4 A). However, at 280 min⁻¹ the use of middle sized (\sim 170 µm), or large sized (\sim 870 µm) beads significantly decreased the yield as compared to 180 min⁻¹ to a maximum ThT-Fl. of 10.8 A.U (Fig. 3 C). and 8.8 A.U (Fig. 3 E). after 5 h, respectively.

The same experiment at pH 3.5 led only to a slightly higher increase in ThT-Fl. compared with pH 2 when glass beads were used (Fig. 3 F - J). Shaking at 180 min $^{-1}$ without beads led to a ThT-Fl. increase of 4.3 \pm 0.3 A.U. to 8.6 \pm 1.2, while after 5 h with beads ThT-Fl. of 9.8 A.U. (~170 μ m), 9.9 A.U. (~520 μ m) or 9.5 A.U. (~870 μ m) were achieved (Table 3). The use of ~6.6 μ m beads led to protein precipitation after ~4 h. In the course of incubation, the solution got turbid, which made an adequate measurement of the sample after 5 h impossible (Fig. 3 G). Turbidity was not observed for pH 2 solutions.

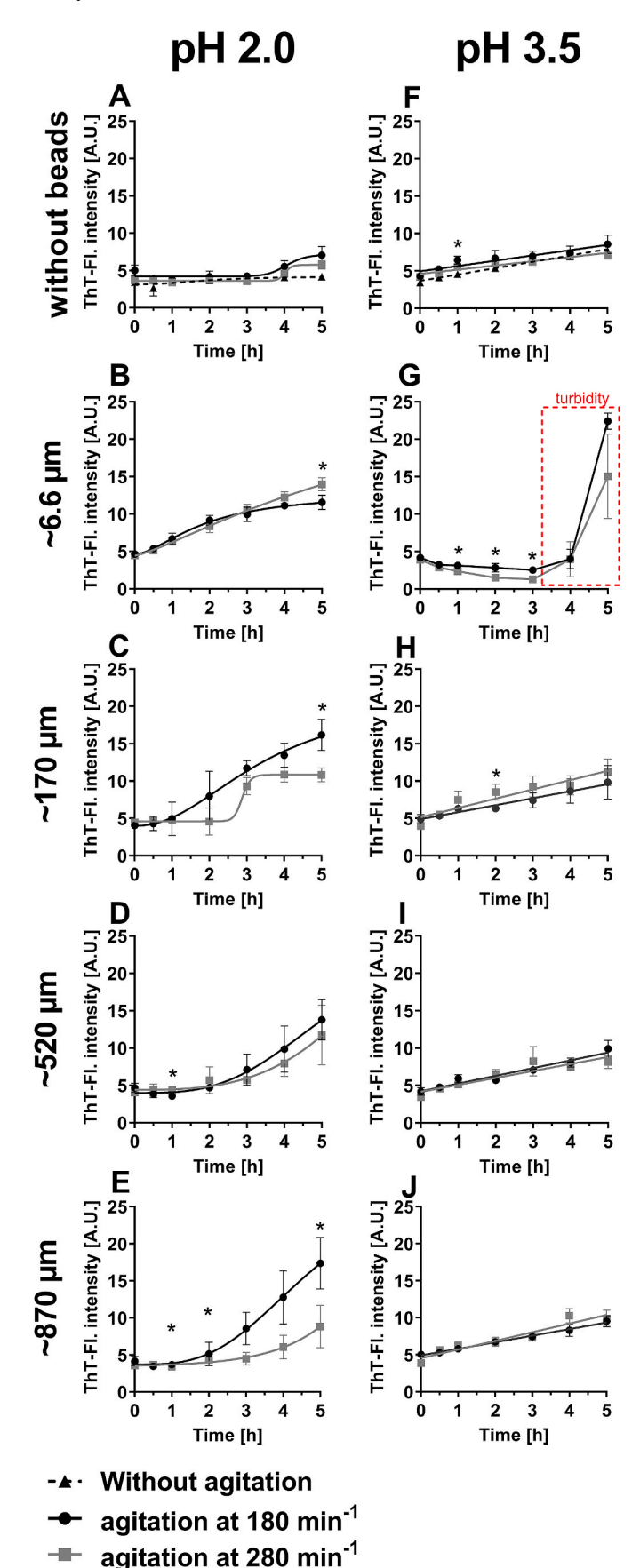
For the BLG solutions at pH 3.5, an increase of the shaking speed to 280 min $^{-1}$ led to few changes in the ThT-Fl.: After 5 h: 7.1 A.U. (without beads), 11.2 A.U. (\sim 170 μ m), 8.1 A.U. (\sim 520 μ m), 9.9 A.U. (\sim 870 μ m) (Fig. 3 F and H - J). Again, the \sim 6.6 μ m beads caused precipitation of the protein, and thus turbidity of the solution (Fig. 3 G).

Different particle sizes and different agitation velocities led to different stress energies: Fig. 4 illustrates the dependence of ThT-Fl. on the respective stress energy at pH 2 and \sim 70 °C protein solution.

Higher shaking frequencies of 280 min^{-1} led to lower ThT-Fl. (8.8 A. U. [$\sim 870 \text{ }\mu\text{m}$]; 11.8 A.U. [$\sim 520 \text{ }\mu\text{m}$] than lower shaking frequencies of 180 min^{-1} (ThT-Fl. 17.4 A.U. [$\sim 870 \text{ }\mu\text{m}$]; 13.8 A.U. [$\sim 520 \text{ }\mu\text{m}$]). The bead power input (W) is the product of the stress frequency (s^{-1}) and the mean stress energy (J) and is introduced by the bead to bead (BB) collision or the bead power input which is generated by the movement of the beads over the flask bottom or the flask wall (BW). The bead power input was higher for the agitated systems with coarser glass beads ($\sim 870 \text{ }\mu\text{m}$) than for smaller glass beads ($\sim 520 \text{ }\mu\text{m}$) (807 J vs 379 W). Focusing on the type and the location of the stress contact, it was found that the shear stress during BW contacts strongly dominates over the normal stress (by the factor of 5-8), and has a higher value at a shaking frequency of 280 min^{-1} ($164 \text{ W } [\sim 870 \text{ }\mu\text{m}]$; $99 \text{ W } [\sim 520 \text{ }\mu\text{m}]$), compared to shaking frequencies of 180 min^{-1} ($111 \text{ W } [\sim 870 \text{ }\mu\text{m}]$; $57 \text{ W } [\sim 520 \text{ }\mu\text{m}]$).

The investigation of the aggregate morphology confirmed a formation of strand-like fibrils at pH 2 when beads larger than 100 μm were added (Fig. 5 A - C). In all experiments, a very short protein aggregate contour length of 1 μm maximum at an average length of $\sim\!370\pm220$ nm was evident, as was the presence of many very short protein particles $<\!100$ nm. At a pH value of 3.5, barely completed worm-like aggregates were found (Fig. 5 D – F). The present aggregates had an average length of $\sim\!42\pm17$ nm. In addition, numerous protein particles of $<\!10$ nm were observed.

T.R. Heyn et al. Food Hydrocolloids 139 (2023) 108511



(caption on next column)

Fig. 3. Influence of glass beads with different mean diameters (no glass beads: A & F; 6,6 μ m: B & C; 170 μ m: C & H; 520 μ m: D & I; 870 μ m: E & J) in the shaking flasks on the amyloid aggregation kinetics of beta-lactoglobulin at \sim 70 °C solution temperature measured with ThT-fluorescence assay (ThT-Fl. intensity) over 5 h. The ThT-assay quantifies the amount of amyloid structure in the protein solution and is independent from aggregate length (Heyn et al., 2021). Protein solutions were adjusted to pH 2.0 (A–F) or 3.5 (F–J) and agitated at 0 min $^{-1}$, 180 min $^{-1}$ or 280 min $^{-1}$. Significant differences in ThT-Fl. between shaking frequencies were marked with *. The aggregation kinetics was fitted with a sigmoidal equation (Heyn et al., 2020) when using pH 2 (A–E) or linear regression when using pH 3.5 (F & H – J). The growth rate, lag time and r-square of the sigmoidal fits are listed in the supplementary material TAB S3 – S5.

3.3. Influence of particle surface on amyloid aggregation

In order to investigate the influence of the particle surface on amyloid aggregation, the surface chemistry of the glass beads was modified by covalently attaching stearic acid. It was found that the hydrophobic modified surfaces inhibited the amyloid aggregation of BLG (Fig. 6). Thus, at pH 2, the ThT-Fl. increased after 5 h to a maximum of 6.7 \pm 1.3 A.U. (\sim 6.6 µm), 8.9 \pm 0.9 A.U. (\sim 170 µm), 7.6 \pm 1.0 A.U. (\sim 520 µm) and 7.8 \pm 1.8 A.U. (~870 $\mu m).$ These fluorescence intensities were all significantly lower than for unmodified glass beads (Fig. 6 A - D). At pH 3.5, the application of the modified \sim 520 μm glass beads led to only small differences with respect to protein aggregate formation (Fig. 6 G) (i.e.ThT-Fl. of 7.5 \pm 0.5 A.U. instead of 8.1 A.U for the unmodified glass beads). The analysis of the free protein concentration in solution by UV/ VIS (see supporting information TAB S2) revealed a strong protein adsorption to the unmodified \sim 6.6 μ m beads at pH 3.5, and an increased occurrence of turbidity in the protein solution after 4 h (Fig. 6 E). Interestingly, modified beads with \sim 6.6 μm diameter seemed to adsorb protein without causing turbidity in the solution.

If the modified beads with ${\sim}6.6~\mu m$ were used at pH 2, the AFM analysis (Fig. 7 A) illustrated not only the sporadic presence of strand-like fibrils with a length of ${\sim}400\pm130$ nm, but also a large number of worm-like aggregates with a length of ${\sim}55\pm17$ nm. Modified beads with a diameter of ${\sim}170~\mu m$ did not cause worm-like structures at pH 2, but led to strand-like fibrils of ${\sim}500\pm250$ nm length (Fig. 7 B). The high adsorption of protein at pH 3.5 to the ${\sim}6.6~\mu m$ beads led to a high loss of protein in the solution, which was also shown by the fact that no protein aggregates were detected by AFM (Fig. 7 C). At pH 3.5, no significant adsorption to the ${\sim}170~\mu m$ beads was measured and worm-like morphologies of ${\sim}60\pm21$ nm contour length could be observed (Fig. 7 D).

4. Discussion

4.1. Effect of glass bead size and agitation on amyloid aggregation

To investigate the effect of glass beads on the aggregation kinetics of BLG and on the resulting morphology of these aggregates, different bead sizes and agitation velocities were tested. When glass beads of $\sim\!870~\mu m$ diameter were used at a pH-value of 2, the yield of fibril formation, based on the ThT-assay, after 5 h was higher than in the standard experiments using a magnetic stirrer under comparable conditions (same pH-value, same protein and same protein-concentration) (Heyn et al., 2020). The BLG solution processed by agitation with beads at a mean temperature of 69.2 °C had a ThT-Fl. of approx. 17. A.U. (Table 3), while stirring reached only approx. 3 A.U. Similarly high ThT-Fl. values of approx. 18. A.U. were achieved by stirring at a higher temperature of 75 °C. Accordingly, the use of beads during agitation (stirring, shearing) can increase the aggregation kinetics of BLG in a lower temperature range, and could thus allow a process temperature reduction of 5 K. AFM analyses confirm the presence of fibrils in the bead system at 70 °C. However, the AFM analyses also gave evidence of a fragmentation of the

Table 3 Overview of the influence of glass bead variants on fibril yield (ThT-Fl.), aggregation kinetics (lag-phase), morphology (Contour length) and adsorption to the particle surface, when pH 2 or pH 3.5 protein solution were agitated at 180 min $^{-1}$ and \sim 70 °C.

pH value Glass bead surface		pH2	pH2			pH3.5	
		unmodified	Stearic acid modified	NaOH treated	unmodified	Stearic acid modified	
Glass bead size [µm]		maximal ThT-F	maximal ThT-Fl. [A.U.] at 180 min ⁻¹				
~870		17.4	8.9	9.4	9.9	9.3	
		lag phase*					
~6.6		_	++	n.r.	_	n.r.	
~170		+	++	n.r.	_	_	
~520		++	++	++	_	_	
~870		++	++	++	-	-	
		contour-length	[nm]				
~6.6		n.r.	\sim 400 \pm 130	n.r.	n.r.	${\sim}55\pm17$	
~170		$\sim\!335\pm230$	\sim 500 \pm 250	n.r.	${\sim}42\pm17$	\sim 60 \pm 21	
~520		${\sim}460\pm280$	n.r.	n.r.	$\sim \! 38 \pm 15$	n.r.	
~870		$\sim\!310\pm170$	n.r.	n.r.	$\sim \! 37 \pm 15$	n.r.	
	protein association status	adsorption *					
~6.6	aggregates	-	+	n.r.	++	++	
	monomers/dimers	++	+	n.r.	++	+	

^{* (-)} non-existent/low; (+) existent/increased: (++) highly visible/high; (n.r.) no results available.

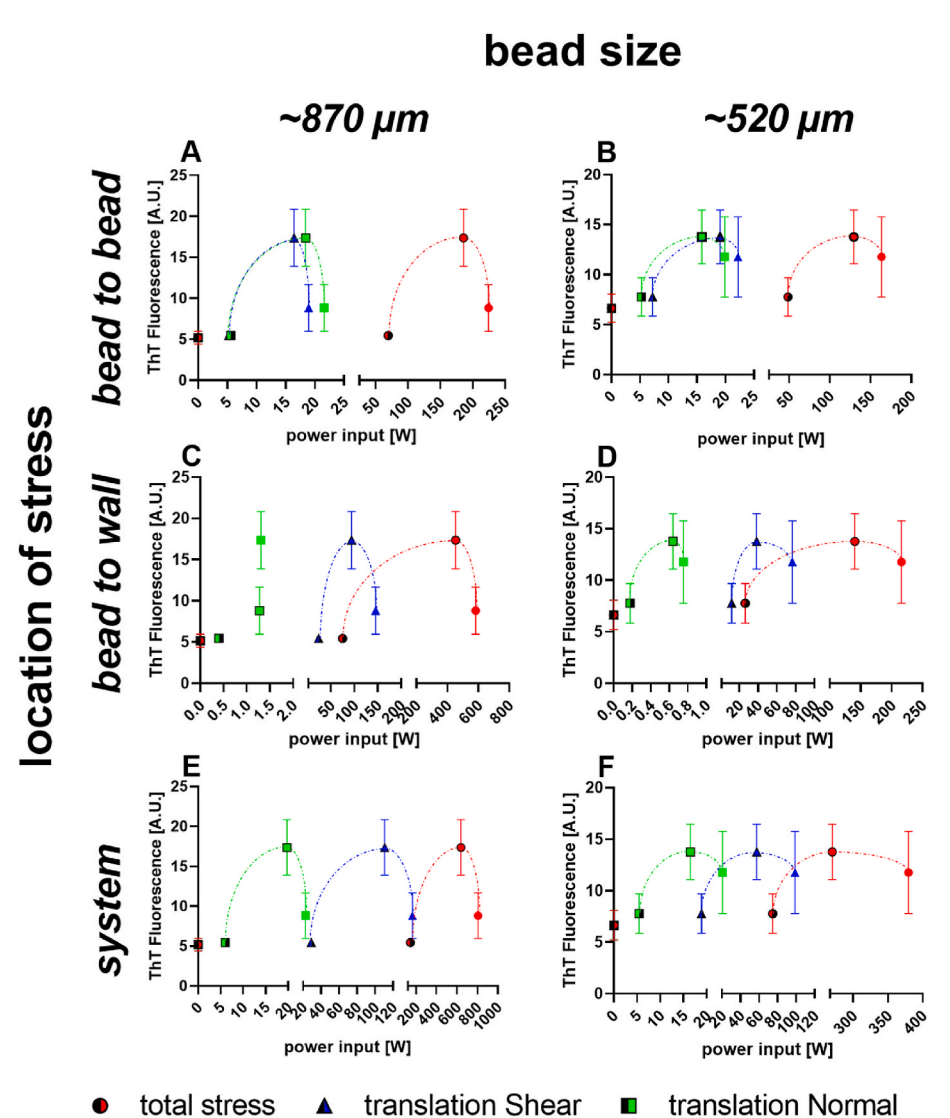


Fig. 4. Increase of ThT-Fl. in pH 2 solutions after 5 h depending on the bead power input in the presence of unmodified glass beads with diameter of ${\sim}870~\mu m$ vs. ${\sim}520~\mu m$ at different shaking frequencies (60 $\min^{-1} \mathbf{I}$, 120 $\min^{-1} \mathbf{I}$, 180 $\min^{-1} \mathbf{I}$, 280 $\min^{-1} \mathbf{I}$). Stress power input was calculated out of CFD-DEM simulations and is the product of stress frequency and mean stress energy. Here it was differentiated according to the type of stress contact (total stress, translational normal and translational shear) and the locality of the collision (bead to bead/bead to wall). The stress energy calculated for the whole system is the average of the sum of the stress energies for bead to bead and bead to wall contacts. The dotted line presents the parabolic relationship between stress energy and fibril formation. The power input at shaking frequencies of 60 $\mbox{min}^{-1} < 0.01 \mbox{ W}.$

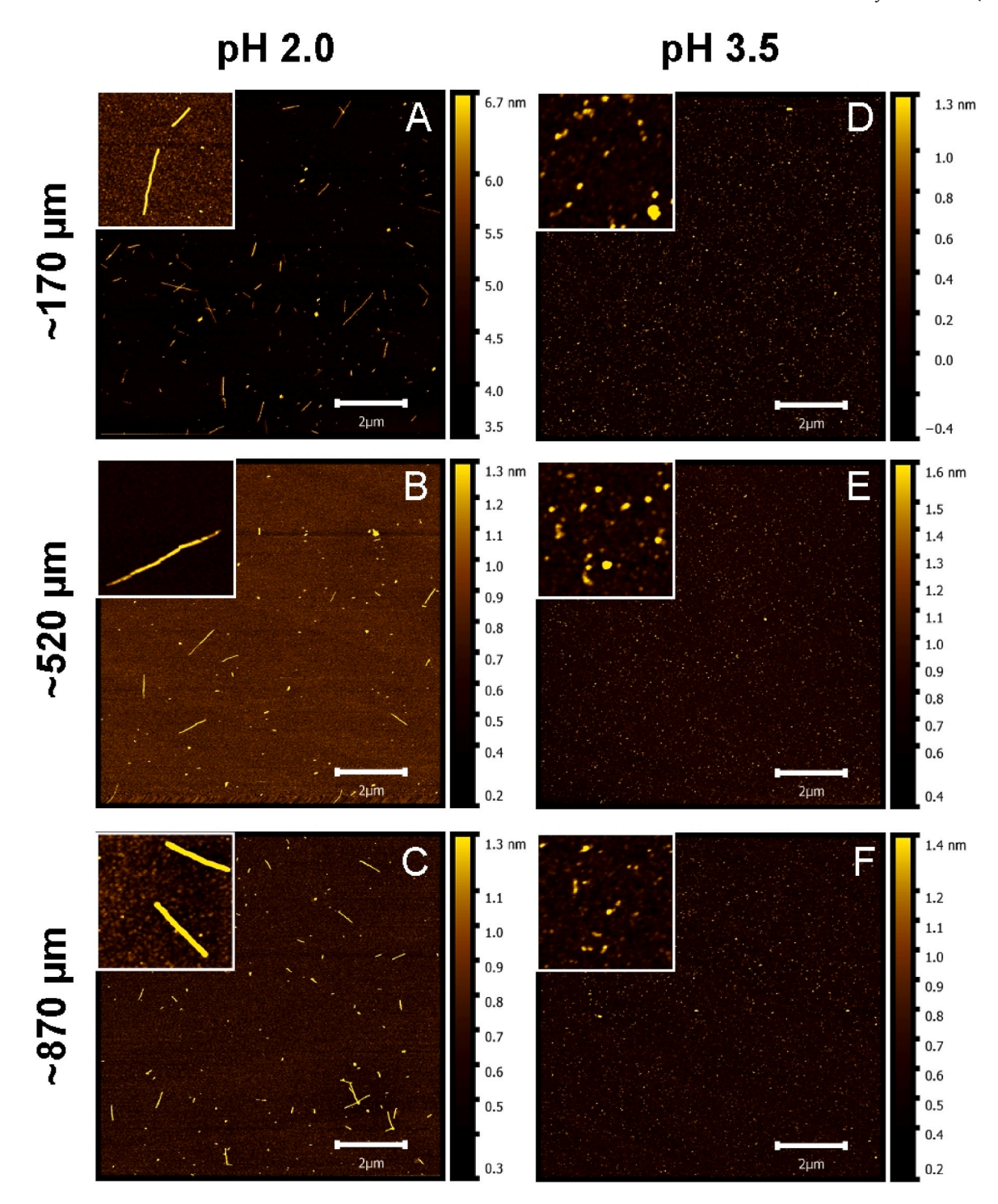


Fig. 5. Atomic force microscopy images of samples with 0.01 wt% beta-lactoglobulin after 5 h at \sim 70 °C. Samples were agitated at 180 min⁻¹ with unmodified glass beads of different diameter and at different pH values. (A) Diameter of \sim 170 μ m and pH 2. (B) Diameter of \sim 520 μ m and pH 2. (C) Diameter of \sim 870 μ m and pH 3.5. (E) Diameter of \sim 520 μ m and pH 3.5. (E) Diameter of \sim 520 μ m and pH 3.5. Edge length of the white squares is 0.5–1 μ m.

bead-induced fibrils, so that a shorter contour length of \sim 0.5 µm (Fig. 5 A to C/TAB 3) was achieved compared with conventional fibrils of >7 µm (Heyn et al., 2019). Previous results have shown that the ThT-Fl. is independent of the fibril length distribution (Heyn et al., 2021). However, the high aspect ratio of fibrils is an important characteristic in terms of different applications (e.g. gelling properties, surface adsorption etc.). Though in most applications, the fibrils are comminuted along the processing (Heyn et al., 2021). For some applications, smaller fibrils length even might have advantages (e.g. higher diffusion speeds to

interfaces).

Despite the acceleration effect on the fibril formation of BLG at pH 2, the aggregation into worm-like amyloid aggregates at pH 3.5 seems to be independent from the addition of glass beads and agitation velocity.

The processing of protein solutions at pH 3.5 with glass beads led to a direct increase of the ThT-Fl within minutes of the process. Therefore, no lag phase was evident at pH 3.5 (Fig. 3 F - J) in contrast to pH 2 solutions, where an increase of ThT-Fl. occurred with a lag time when no bead, or beads $>400 \mu m$ were used (Fig. 3 C to E). This pH 2 lag phase is

T.R. Heyn et al. Food Hydrocolloids 139 (2023) 108511

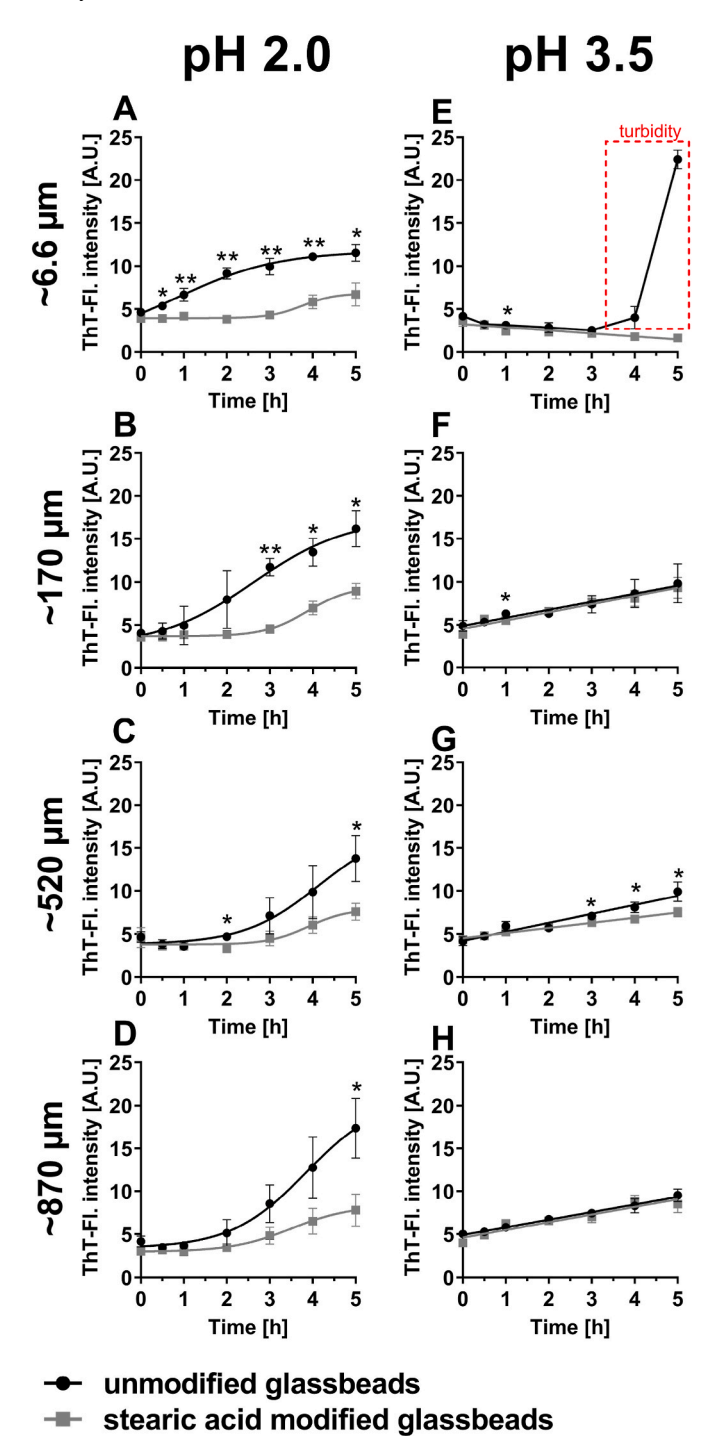


Fig. 6. Influence of stearic acid surface modified glass beads with different mean diameters (6.6 μm : A & E; 170 μm : B & F; 520 μm : C & G; 870 μm : D & H) on the amyloid aggregation of beta-lactoglobulin at $\sim\!70$ °C measured with ThT-Fl. assay over 5 h. The ThT-assay quantifies the amount of amyloid structure in the protein solution and is independent from aggregate length (Heyn et al., 2021). Protein solutions were adjusted to pH 2.0 (A – D) or pH 3.5 (E – H) and agitated at 180 min $^{-1}$. The results for unmodified glass beads correspond to the data in Fig. 3. Significant differences in THT-Fl. between different treated glass beads were marked with *. The aggregation kinetics was fitted with a sigmoidal equation (Heyn et al., 2020) when using pH 2 (A – D) or linear regression when using pH 3.5 (E – H). The growth rate, lag time and r-square of the sigmoidal fits are listed in the supplementary material TAB S4 & S6.

based on the provision of the self-assembling peptide building blocks for the fibrils by acid hydrolysis of BLG, and represents the initial nucleus phase of the amyloid aggregates (Akkermans et al., 2006; Dave et al., 2013). A different aggregation mechanism of amyloid-like aggregates at pH values \geq 3.35, where intact BLG forms the self-associating building blocks due to reduced acid hydrolysis, has already been discussed previously (Heyn et al., 2019; Prashant Mudgal, Daubert, & Foegeding, 2011; Serfert et al., 2014). A comparison with unpublished data indicates a slightly higher aggregation kinetics for these agitated samples compared to stirred protein solutions at pH 3.5. The AFM analysis demonstrated that in the agitation vessel with beads only fragments of worm-like aggregates were formed (Fig. 5 D - F), which contrasts with the described length of 50-200 nm of the conventional worm-like aggregates induced by magnetic stirring at similar conditions but higher temperature (Heyn et al., 2019; Serfert et al., 2014). This indicates a lower mechanical stability of the worm-like BLG aggregates compared with the fibrils, as reported previously (Heyn et al., 2019).

The increased fibril formation occurring at larger bead sizes (>400 μm) at pH 2 is possibly based on the physical energy input of the beads to the protein by shear, impact and rolling movement (Schrader et al., 2019). According to the literature, the input of shear forces accelerates fibril formation by carrying building blocks to the fibril tips (Akkermans et al., 2008), or by fragmentation of already formed protofibrils into seeds and a subsequent secondary nucleation (Dunstan et al., 2009). That this effect is of great relevance here could be deduced from the high apparent degree of fragmentation of fibrils at pH 2 as well as the deterioration of amyloid-like aggregates at pH 3.5 (Fig. 6). At the same time, this finding confirms once again that the formation of amyloid-like aggregates at pH 3.5 is independent of nucleation, since despite visible fragments no acceleration of the aggregation is apparent (Fig. 3 H - J). (Akkermans et al., 2008) have already shown that there is a parabolic relationship between fibril formation kinetics and shear input. The CFD-DEM results shown in Fig. 4 can further differentiate this dependence into the different types of stress acting on the aggregates: Too high agitation velocities had an adverse effect on the BLG fibril formation. The CFD-DEM simulation found an increased bead power input due to increased mean stress energy and stress frequency (see appendix) at increasing shaking frequencies. Next to the total stress, which calculation bases on different contact types (Schrader et al., 2019), the shear stress due to bead to wall contacts seems to dominate over other contact types. Although the stress frequency of bead to bead contacts seems to be higher by a factor of 10. Therefore, it can be suggested that at higher agitation velocities the shear stress becomes too high, resulting in a parabolic relationship between shear and fibril formation as it was mentioned by Akkermans et al. (2008) after investigations with a shearing device (Couette geometry). However, the kinetics of fibril formation does not appear to be in direct relationship with the measured bead power input value: The fibril formation with $\sim\!870~\mu m$ beads was highest at 638 W and decreased at 806 W, whereas with \sim 520 μ m beads, the highest fibril formation was found at a bead power input value of 270 W and decreased at 379 W. Therefore, other factors such as surface area of the glass beads and laminar and turbulent flow behaviour of the water (Heyn et al., 2020) (supporting information MOV S1) might also have an impact.

In the case of smaller beads, the lag phase of the fibril formation at pH 2 is minimized (Table 3). This observation may be attributed to the specific surface area at this particle size, which is large enough to enable "surface-assisted nucleation" effects (Linse et al., 2007; Pronchik et al., 2010). This promoting of the aggregation by the primary heterogeneous nucleation effect was described by (Linse et al., 2007) for the aggregation of beta₂-microglobulin, when using copolymeric nanoparticles (Linse et al., 2007), which was later confirmed by (Grigolato et al., 2017) for the amyloid aggregation on human insulin with polymeric nanoparticles in combination with hydrodynamic flow and mechanical agitation. Known effects related to amyloid aggregation are the increase of the local concentration of the proteins at particle surfaces and their

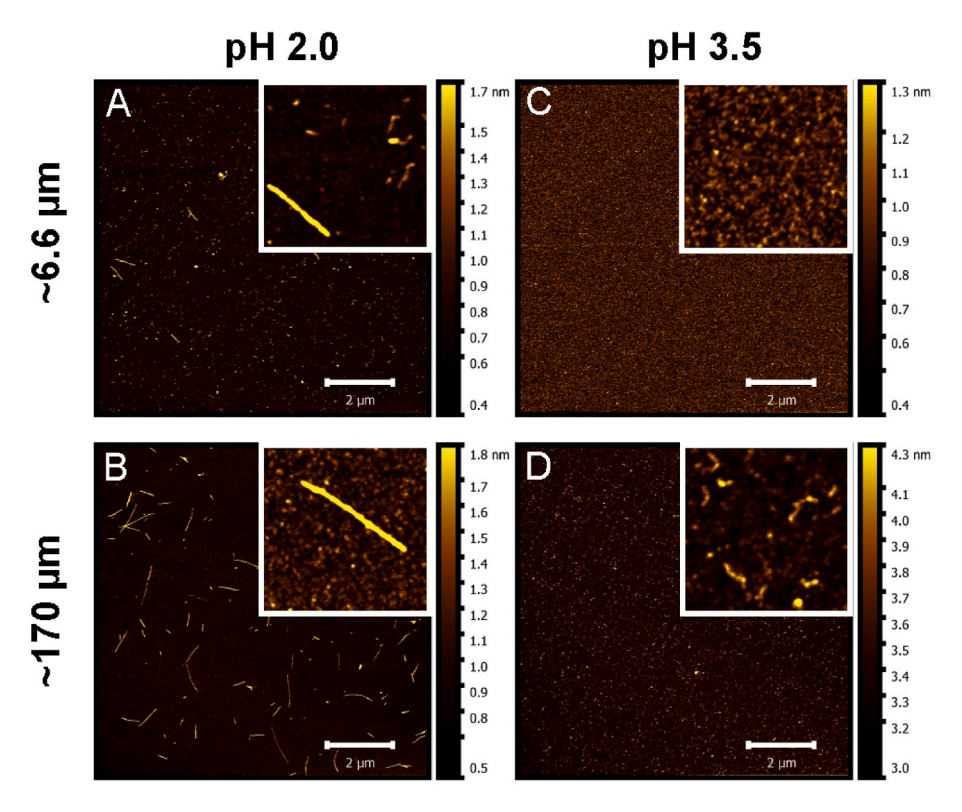


Fig. 7. Atomic force microscopy images of samples with 0.01 wt% beta-lactoglobulin samples after 5 h at \sim 70 °C. Samples were agitated at 180 min⁻¹ with stearic modified glass beads of different diameter and at different pH values. (A) Diameter of \sim 6.6 μ m and pH 2. (B) Diameter of \sim 170 μ m and pH 2. (C) Diameter of \sim 6.6 μ m and pH 3.5. (D) Diameter of \sim 170 μ m and pH 3.5.

subsequent association into a two dimensional area (Shezad et al., 2016). Further effects may be protein destabilization (Perriman et al., 2007), or unfolding (Marengo et al., 2016) at the interfaces, which can increase the protein hydrolysis kinetics by exposing acid cleavable asparagine-linked peptides (van der Linden & Venema, 2007). Although significant protein (or fibril) adsorption on the glass beads was not evident with FTIR (Fig. 1 B), these effects could also be relevant in case of temporary adsorption, as it has been described for the formation of alpha-synuclein fibrils (Pronchik et al., 2010; Shezad et al., 2016) or human insulin (Grigolato et al., 2017). As mentioned by (Grigolato & Arosio, 2021) the results highlight the synergistic role of the surface effects and the hydrodynamic flow and mechanical stress, which enhances primary nucleation, accelerating mass transport and promote secondary nucleation.

4.2. Effect of glass particle surface on amyloid aggregation

4.2.1. Adsorption effects

To test the effect of interfaces on the fibril formation of BLG, the particle surfaces were chemically modified with stearic acid. The analysis of the glass beads by ATR-FTIR showed the successful binding of stearic acid to the glass bead surface (Fig. 1). The FTIR analysis of the protein-specific Amide I and II bands also revealed BLG adsorption to the glass bead surface after the beads were incubated for 5 h in pH 2 or pH 3.5 protein solution: The aggregates formed at pH 3.5 showed a typical Amide I shoulder at 1620 cm⁻¹, indicating the presence of intermolecular beta-sheets (i.e. aggregates) on the bead surface irrespective of the surface modification (Kavanagh et al., 2000b). However, at pH 2, this shoulder only occurred when stearic acid modified beads were used, indicating that fibrillar BLG does not adhere to the unmodified glass surface, but to the hydrophobic surface. Since silicon dioxide - which is the main constituent of glass beads - has a zeta potential of 0 mV at a pH between 3.5 and 4.0 (Ali et al., 2022), it can be assumed that the

increased adsorption of the BLG on the surface of the bead is favoured by the low charge effects (Ali et al., 2022), demonstrated the complexity of the silica (SiO₂) particle – protein (bovine serum albumine) interaction. The authors suggested that positive charged amino acids of the protein might interact with the silica surface, but also led to complexation with dissolved silicate species. It can be expected that the content of dissolved Na-ions increases with time and elevates the pH-value of the solution (Maraghechi, Rajabipour, Pantano, & Burgos, 2016), which would be an explanation for the precipitated protein solution (Fig. 3 G) when using the smallest glass beads (\sim 6.6 μ m) with a maximum of ions releasing specific surface area. At pH values < 3, the positive charge of both, SiO₂ and BLG (Heyn et al., 2019), lead to electrostatic repulsive forces, which might inhibit the interfacial attachment of BLG at pH 2. If stearic acid-modified surfaces were used, repulsions was hindered, since stearic acid might lower the zeta potential of surfaces (Derkani et al., 2019). Additionally, due to their high stiffness and aspect-ratio (Adamcik et al., 2010), fibrillar aggregates may offer large targets for the shear flow and are thus easily removed from the particle surface by shear forces. The stearic acid modified bead surfaces (Fig. 1 A) in turn provide hydrophobic anchor points, from which larger fibrils cannot be removed by the shear flow this easily. It was mentioned by (Grigolato & Arosio, 2021), that the morphological complexity of surfaces plays an important role for interactions between surface and protein. This phenomenon was described for the interaction of amyloid polypeptide with star polymers (Pilkington et al., 2017) or for human insulin with chiral silica nanoribbons (Sukhanova et al., 2019). In contrast to pH 2, the worm-like and much smaller structures at pH 3.5 probably remained on the smooth unmodified glass surfaces due to their small surface area and lower surface charge (Heyn et al., 2019; Prashant Mudgal, Daubert, & Foegeding, 2011; Serfert et al., 2014). This adsorption phenomenon also indicates specific interfacial functionalities of pH 3.5 aggregates.

4.2.2. Aggregation kinetics

The use of stearic acid modified glass beads lowered the fibrillation rate in pH 2 solution compared with the use of unmodified glass beads. For the smallest bead sizes <200 μm , the presence of the lag phase was evident again (Fig. 6 A/TAB 3). As shown exemplarily for the \sim 870 μm beads, also the initial treatment with NaOH led to a decrease of the aggregation kinetics. Possibly the modification causes several effects, which inhibit the nucleation enhancing properties. In addition to the chemical alteration, the beads also changed their physical surface properties in the course of particle modification. The 15 min activation step using 4 M NaOH solution resulted in the removal of the surface relief on the glass beads (Fig. 2). An alteration of the glass particle surfaces by NaOH treatment was described before (Ozmen et al., 2009). The change in physical surface properties can alter the friction, shear or impact forces acting between the beads and, thus, have an influence on the mechanical energy input. Modification with stearic acid led to an altered particle surface, with different characteristics for different particle sizes (Fig. 2 C). In addition, a change in surface hardness and – as mentioned before - the charge could be possible, but has not been tested here.

The increase in particle hydrophobicity in the course of stearic acid bonding might also have altered the described adsorption behaviour of BLG (Pronchik et al., 2010) or 2D diffusion at the surface (Shezad et al., 2016), which would explain the reoccurrence of a lag-phase for the smallest beads (Fig. 6 B/TAB 3). Non-covalent interactions between the particle surface bound fatty acid residues and the BLG, especially with the cavity of BLG, are also conceivable (Loch et al., 2012). Although BLGs affinity to saturated fatty acids is very low at pH values < 4.5 (Frapin et al., 1993). However, the affinity of BLG to fatty acids can be different in denatured, aggregated or hydrolysed state (Le Maux et al., 2014). In fact, the ATR-FTIR investigations revealed a lower intensity at pH 2 and at pH 3.5 for protein at the modified glass bead surface in general (Fig. 1 B), compared to the unmodified surface. However, at the modified surface, the presence of aggregated material was evident at pH 2, indicating that fibrils are more likely to attach to hydrophobic surfaces, which corresponds to the surface active character of the fibrils to oil- and air-water interfaces (Gao et al., 2017; Moro et al., 2013; Serfert et al., 2014).

5. Conclusion

The investigations performed in this study primarily show that the addition of glass beads enhanced the fibril formation of BLG at pH 2, while the aggregates formed at pH 3.5 were not affected in their aggregation kinetics. The glass beads with a diameter ≥170 µm primarily affected the BLG fibril formation through additional mechanical energy input, and the fibril aggregation kinetics was in turn accelerated by enhanced secondary nucleation. However, this effect resulted in the formation of shorter fibrils and aggregate lengths than in a stirring process, probably because fibrils were fragmented during or after their formation. Based on CFD-DEM simulation, the translational shear stress, due to bead-to-wall contacts, could be the decisive factor for the increased fibril formation in systems agitated with glass beads. Overall, the application of glass beads in a shaken flask accelerated fibril formation compared to a stirred system, potentially saving heating energy. Especially collision loads seem to have a promoting effect. However, glass bead assisted fibril formation systems may lead to smaller fibril length and thus a loss of the high aspect ratio, an important feature of fibrils. The smallest glass beads used offered a sufficiently large surface area to support the nucleation of fibrils during the lag-phase by interface effects. The covalent bonding of stearic acid to the glass beads led to a strong reduction of these supportive effects. Thus, smooth and more hydrophilic surfaces are more advantageous for enhancing particle or fibril formation. Various aggregate forms have different affinities to surfaces with distinct properties. This insight can be used to derive areas of application for specific aggregate morphologies or to separate specific morphologies from a heterogenous system. More detailed knowledge should be gained in the future on the influence of different surface types (polymers, carboxylic acids of different lengths, etc.), heterogeneous particle mixtures and varying protein-glass bead ratios.

CRediT author statement

Timon R. Heyn: Conceptualization, Methodology, Formal analysis, Investigation, Validation, Visualization, Writing - Original Draft, Marcel Schrader: Methodology, Investigation, Formal analysis, Validation, Writing - Original Draft, Visualization, Ingo Kampen: Resources, Validation, Writing - Review & Editing, Arno Kwade: Resources, Supervision, Writing - Review & Editing, Karin Schwarz: Project administration, Funding acquisition, Conceptualization, Resources, Writing - Review & Editing, Supervision, Julia K. Keppler: Project administration, Conceptualization, Funding acquisition, Resources, Writing - Review & Editing, Supervision.

Conflict of interest

None.

Declaration of competing interest

None.

Data availability

Data will be made available on request.

Acknowledgement

This project was funded by DFG SPP 1934 DisPBiotech (Project no. 315456892 and 315460011). We are grateful to Lisiane Petersen and Jesco Reimers of the Food Technology Division Kiel for skilful help in the lab, as well as to Stephanie Michel from the Institute for Particle Technology for conducting the AFM measurements and Kathrin Schrinner from the Institute of Biochemical Engineering in Braunschweig for providing the shake flasks. The authors would like to acknowledge Wolfgang Voit from Sigmund Lindner GmbH for the kind provision of the glass beads.

Appendix A. Supplementary data

Supplementary data to this article can be found online at https://doi.org/10.1016/j.foodhyd.2023.108511.

References

- vandenAkker, C. C., Schleeger, M., Bruinen, A. L., Deckert-Gaudig, T., Velikov, K. P., Heeren, R. M. A., Deckert, V., Bonn, M., & Koenderink, G. H. (2016). Multimodal spectroscopic study of amyloid fibril polymorphism. *Journal of Physical Chemistry B*, 120(34), 8809–8817. https://doi.org/10.1021/acs.jpcb.6b05339
- Adamcik, J., Jung, J.-M., Flakowski, J., Los Rios, P. de, Dietler, G., & Mezzenga, R. (2010). Understanding amyloid aggregation by statistical analysis of atomic force microscopy images. *Nature Nanotechnology*, 5(6), 423–428. https://doi.org/10.1038/nnano.2010.59
- Akkermans, C., van der Goot, A. J., Venema, P., van der Linden, E., & Boom, R. M. (2008). Formation of fibrillar whey protein aggregates: Influence of heat and shear treatment, and resulting rheology. Food Hydrocolloids, 22(7), 1315–1325. https:// doi.org/10.1016/j.foodhyd.2007.07.001
- Akkermans, C., Venema, P., Rogers, S. S., van der Goot, A. J., Boom, R. M., & van der Linden, E. (2006). Shear pulses nucleate fibril aggregation. Food Biophysics, 1(3), 144–150. https://doi.org/10.1007/s11483-006-9012-5
- Ali, M. S., Uttinger, M. J., Romeis, S., Schmidt, J., & Peukert, W. (2022). Effect of protein adsorption on the dissolution kinetics of silica nanoparticles. *Colloids and Surfaces, B: Biointerfaces*, 214, Article 112466. https://doi.org/10.1016/j.colsurfb.2022.112466
- Bolder, S. G., Sagis, L. M. C., Venema, P., & van der Linden, E. (2007). Effect of stirring and seeding on whey protein fibril formation. *Journal of Agricultural and Food Chemistry*, 55(14), 5661–5669. https://doi.org/10.1021/jf063351r

T.R. Heyn et al. Food Hydrocolloids 139 (2023) 108511

Bolisetty, S., Adamcik, J., Heier, J., & Mezzenga, R. (2012). Amyloid directed synthesis of titanium dioxide nanowires and their applications in hybrid photovoltaic devices. Advanced Functional Materials, 22(16), 3424–3428. https://doi.org/10.1002/ adfm 201103054

- Bolisetty, S., Arcari, M., Adamcik, J., & Mezzenga, R. (2015). Hybrid amyloid membranes for continuous flow catalysis. *Langmuir: The ACS Journal of Surfaces and Colloids*, 31 (51), 13867–13873. https://doi.org/10.1021/acs.langmuir.5b03205
- Bolisetty, S., Boddupalli, C. S., Handschin, S., Chaitanya, K., Adamcik, J., Saito, Y., Manz, M. G., & Mezzenga, R. (2014). Amyloid fibrils enhance transport of metal nanoparticles in living cells and induced cytotoxicity. *Biomacromolecules*, 15(7), 2793–2799. https://doi.org/10.1021/bm500647n
- Cao, Y., & Mezzenga, R. (2019). Food protein amyloid fibrils: Origin, structure, formation, characterization, applications and health implications. Advances in Colloid and Interface Science, 269, 334–356. https://doi.org/10.1016/j.cis.2019.05.002
- Dave, A. C., Loveday, S. M., Anema, S. G., Loo, T. S., Norris, G. E., Jameson, G. B., & Singh, H. (2013). B-lactoglobulin self-assembly: Structural changes in early stages and disulfide bonding in fibrils. *Journal of Agricultural and Food Chemistry*, 61(32), 7817–7828. https://doi.org/10.1021/jf401084f
- Derkani, M. H., Fletcher, A. J., Fedorov, M., Abdallah, W., Sauerer, B., Anderson, J., & Zhang, Z. J. (2019). Mechanisms of surface charge modification of carbonates in aqueous electrolyte solutions. *Colloids and Interfaces*, 3(4), 62. https://doi.org/ 10.3390/colloids3040062
- Dunstan, D. E., Hamilton-Brown, P., Asimakis, P., Ducker, W., & Bertolini, J. (2009). Shear-induced structure and mechanics of β-lactoglobulin amyloid fibrils. Soft Matter, 5(24), 5020. https://doi.org/10.1039/b914089a
- Frapin, D., Dufour, E., & Haertle, T. (1993). Probing the fatty acid binding site of betalactoglobulins. *Journal of Protein Chemistry*, 12(4), 443–449. https://doi.org/
- Gao, Z., Zhao, J., Huang, Y., Yao, X., Zhang, K., Fang, Y., Nishinari, K., Phillips, G. O., Jiang, F., & Yang, H. (2017). Edible Pickering emulsion stabilized by protein fibrils. Part 1: Effects of pH and fibrils concentration. LWT - Food Science and Technology, 76, 1–8. https://doi.org/10.1016/j.lwt.2016.10.038
- Goniva, C., Kloss, C., Deen, N. G., Kuipers, J. A., & Pirker, S. (2012). Influence of rolling friction on single spout fluidized bed simulation. *Particuology*, 10(5), 582–591. https://doi.org/10.1016/j.partic.2012.05.002
- Gosal, W. S., Clark, A. H., & Ross-Murphy, S. B. (2004). Fibrillar beta-lactoglobulin gels: Part 3. Dynamic mechanical characterization of solvent-induced systems. *Biomacromolecules*, 5(6), 2430–2438. https://doi.org/10.1021/bm0496615
- Grigolato, F., & Arosio, P. (2021). The role of surfaces on amyloid formation. Biophysical Chemistry, 270(3), Article 106533. https://doi.org/10.1016/j.bpc.2020.106533
- Grigolato, F., Colombo, C., Ferrari, R., Rezabkova, L., & Arosio, P. (2017). Mechanistic origin of the combined effect of surfaces and mechanical agitation on amyloid formation. ACS Nano, 11(11), 11358–11367. https://doi.org/10.1021/acsnano.7b05895
- Heyn, T. R., Garamus, V. M., Neumann, H. R., Uttinger, M. J., Guckeisen, T., Heuer, M., Selhuber-Unkel, C., Peukert, W., & Keppler, J. K. (2019). Influence of the polydispersity of pH 2 and pH 3.5 beta-lactoglobulin amyloid fibril solutions on analytical methods. *European Polymer Journal*, 120, Article 109211. https://doi.org/ 10.1016/j.eurpolymi.2019.08.038
- Heyn, T. R., Mayer, J., Neumann, H. R., Selhuber-Unkel, C., Kwade, A., Schwarz, K., & Keppler, J. K. (2020). The threshold of amyloid aggregation of beta-lactoglobulin: Relevant factor combinations. Journal of Food Engineering, 283, Article 110005. https://doi.org/10.1016/j.ifpodeng.2020.110005
- https://doi.org/10.1016/j.jfoodeng.2020.110005

 Heyn, T. R., Uttinger, M. J., Kwade, A., Peukert, W., Keppler, J. K., & Schwarz, K. (2021).

 Whey protein (amyloid)-aggregates in oil-water systems: The process-related comminution effect. *Journal of Pood Engineering*, 311(6), Article 110730. https://doi.org/10.1016/j.jfoodeng.2021.110730
- Hoppenreijs, L., Fitzner, L., Ruhmlieb, T., Heyn, T. R., Schild, K., van der Goot, A.-J.,
 Boom, R. M., Steffen-Heins, A., Schwarz, K., & Keppler, J. K. (2022). Engineering amyloid and amyloid-like morphologies of β-lactoglobulin. Food Hydrocolloids, 124 (11), Article 107301. https://doi.org/10.1016/j.foodhyd.2021.107301
 Kavanagh, G. M., Clark, A. H., & Ross-Murphy, S. B. (2000a). Heat-induced gelation of
- Kavanagh, G. M., Clark, A. H., & Ross-Murphy, S. B. (2000a). Heat-induced gelation of globular proteins: 4. Gelation kinetics of low pH β-lactoglobulin gels. *Langmuir*, 16 (24), 9584–9594. https://doi.org/10.1021/la0004698
- Kavanagh, G. M., Clark, A. H., & Ross-Murphy, S. B. (2000b). Heat-induced gelation of globular proteins: Part 3. Molecular studies on low pH β-lactoglobulin gels. *International Journal of Biological Macromolecules*, 28(1), 41–50. https://doi.org/ 10.1016/S0141-8130(00)00144-6
- Keppler, J. K., Heyn, T. R., Meissner, P. M., Schrader, K., & Schwarz, K. (2019). Protein oxidation during temperature-induced amyloid aggregation of beta-lactoglobulin. Food Chemistry, 289, 223–231. https://doi.org/10.1016/j.foodchem.2019.02.114
- Kleiber, M., & Joh, R. (Eds.). (2013). VDI-Buch. D3 Stoffwerte von sonstigen reinen Fluiden: Mit 320 Tabellen (11., bearb. und erw. Aufl.). Springer Berlin Heidelberg. https://doi. org/10.1007/978-3-642-19981-3_20.
- Kloss, C., Goniva, C., Hager, A., Amberger, S., & Pirker, S. (2012). Models, algorithms and validation for opensource DEM and CFD-DEM. Progress in Computational Fluid Dynamics, an International Journal, 12(2/3), 140. https://doi.org/10.1504/ PCFD-2012.047457
- Kockmann, A., Hesselbach, J., Zellmer, S., Kwade, A., & Garnweitner, G. (2015). Facile surface tailoring of metal oxide nanoparticles via a two-step modification approach. RSC Advances, 5(75), 60993–60999. https://doi.org/10.1039/C5RA08932H
- Kwade, A.[A. (2003). A stressing model for the description and optimization of grinding processes. Chemical Engineering & Technology, 26(2), 199–205. https://doi.org/ 10.1002/ceat.200390029

Ladner-Keay, C. L., Griffith, B. J., & Wishart, D. S. (2014). Shaking alone induces de novo conversion of recombinant prion proteins to β-sheet rich oligomers and fibrils. PLoS One, 9(6), Article e98753. https://doi.org/10.1371/journal.pone.0098753

- Le Maux, S., Bouhallab, S., Giblin, L., Brodkorb, A., & Croguennec, T. (2014). Bovine β-lactoglobulin/fatty acid complexes: Binding, structural, and biological properties. *Dairy Science & Technology, 94*, 409–426. https://doi.org/10.1007/s13594-014-
- Li, C., Adamcik, J., & Mezzenga, R. (2012). Biodegradable nanocomposites of amyloid fibrils and graphene with shape-memory and enzyme-sensing properties. *Nature Nanotechnology*, 7(7), 421–427. https://doi.org/10.1038/nnano.2012.62
- Li, C., Bolisetty, S., & Mezzenga, R. (2013). Hybrid nanocomposites of gold single-crystal platelets and amyloid fibrils with tunable fluorescence, conductivity, and sensing properties. Advanced Materials, 25(27), 3694–3700. https://doi.org/10.1002/ adma.201300904
- van der Linden, E., & Venema, P. (2007). Self-assembly and aggregation of proteins. Current Opinion in Colloid & Interface Science, 12(4–5), 158–165. https://doi.org/ 10.1016/j.cocis.2007.07.010
- Linse, S., Cabaleiro-Lago, C., Xue, W.-F., Lynch, I., Lindman, S., Thulin, E., Radford, S. E., & Dawson, K. A. (2007). Nucleation of protein fibrillation by nanoparticles. Proceedings of the National Academy of Sciences, 104(21), 8691–8696. https://doi.org/10.1073/pnas.0701250104
- Loch, J. I., Polit, A., Bonarek, P., Olszewska, D., Kurpiewska, K., Dziedzicka-Wasylewska, M., & Lewiński, K. (2012). Structural and thermodynamic studies of binding saturated fatty acids to bovine β-lactoglobulin. *International Journal of Biological Macromolecules*, 50(4), 1095–1102. https://doi.org/10.1016/j.ijbiomac.2012.03.002
- Loveday, S. M., Anema, S. G., & Singh, H. (2017). β-Lactoglobulin nanofibrils: The long and the short of it. *International Dairy Journal*, 67, 35–45. https://doi.org/10.1016/j. idairyj.2016.09.011
- Macchi, F., Hoffmann, S. V., Carlsen, M., Vad, B., Imparato, A., Rischel, C., & Otzen, D. E. (2011). Mechanical stress affects glucagon fibrillation kinetics and fibril structure. *Langmuir : The ACS Journal of Surfaces and Colloids*, 27(20), 12539–12549. https://doi.org/10.1021/la202125c
- Mantovani, R. A., Pinheiro, A. C., Vicente, A. A., & Cunha, R. L. (2017). In vitro digestion of oil-in-water emulsions stabilized by whey protein nanofibrils. Food Research International, 99(Pt 1), 790–798. https://doi.org/10.1016/j.foodres.2017.06.049
- Maraghechi, H., Rajabipour, F., Pantano, C. G., & Burgos, W. D. (2016). Effect of calcium on dissolution and precipitation reactions of amorphous silica at high alkalinity. *Cement and Concrete Research*, 87, 1–13. https://doi.org/10.1016/j. cemconres.2016.05.004
- Marengo, M., Miriani, M., Ferranti, P., Bonomi, F., Iametti, S., & Barbiroli, A. (2016). Structural changes in emulsion-bound bovine beta-lactoglobulin affect its proteolysis and immunoreactivity. *Biochimica et Biophysica Acta, Proteins and Proteomics, 1864* (7), 805–813. https://doi.org/10.1016/j.bbapap.2016.04.007
- Moro, A., Báez, G. D., Ballerini, G. A., Busti, P. A., & Delorenzi, N. J. (2013). Emulsifying and foaming properties of β-lactoglobulin modified by heat treatment. Food Research International, 51(1), 1–7. https://doi.org/10.1016/j.foodres.2012.11.011
- Mudgal, P., Daubert, C. R., Clare, D. A., & Foegeding, E. A. (2011). Effect of disulfide interactions and hydrolysis on the thermal aggregation of β-lactoglobulin. *Journal of Agricultural and Food Chemistry*, 59(5), 1491–1497. https://doi.org/10.1021/ifi01893v
- Mudgal, P., Daubert, C. R., & Foegeding, E. A. (2011). Effects of protein concentration and CaCl2 on cold-set thickening mechanism of β-lactoglobulin at low pH. *International Dairy Journal*, 21(5), 319–326. https://doi.org/10.1016/j. idairyj.2010.11.014
- Ng, S. K., Nyam, K. L., Nehdi, I. A., Chong, G. H., Lai, O. M., & Tan, C. P. (2016). Impact of stirring speed on β-lactoglobulin fibril formation. Food Science and Biotechnology, 25(S1), 15–21. https://doi.org/10.1007/s10068-016-0093-8
- Oboroceanu, D., Wang, L., Magner, E., & Auty, M. A. (2014). Fibrillization of whey proteins improves foaming capacity and foam stability at low protein concentrations. *Journal of Food Engineering*, 121, 102–111. https://doi.org/10.1016/j.ifoodeng.2013.08.023
- Ozmen, M., Can, K., Akin, I., Arslan, G., Tor, A., Cengeloglu, Y., & Ersoz, M. (2009). Surface modification of glass beads with glutaraldehyde: Characterization and their adsorption property for metal ions. *Journal of Hazardous Materials*, 171(1–3), 594–600. https://doi.org/10.1016/j.jhazmat.2009.06.045
- Peng, D., Yang, J., Li, J., Tang, C., & Li, B. (2017). Foams stabilized by β-lactoglobulin amyloid fibrils: Effect of pH. *Journal of Agricultural and Food Chemistry*, 65(48), 10658–10665. https://doi.org/10.1021/acs.jafc.7b03669
- Perriman, A. W., Henderson, M. J., Holt, S. A., & White, J. W. (2007). Effect of the airwater interface on the stability of beta-lactoglobulin. *Journal of Physical Chemistry B*, 111(48), 13527–13537. https://doi.org/10.1021/jp074777r
- Pilkington, E. H., Lai, M., Ge, X., Stanley, W. J., Wang, B., Wang, M., Kakinen, A., Sani, M.-A., Whittaker, M. R., Gurzov, E. N., Ding, F., Quinn, J. F., Davis, T. P., & Ke, P. C. (2017). Star polymers reduce islet amyloid polypeptide toxicity via accelerated amyloid aggregation. *Biomacromolecules*, 18(12), 4249–4260. https://doi.org/10.1021/acs.biomac.7b01301
- Pronchik, J., He, X., Giurleo, J. T., & Talaga, D. S. (2010). In vitro formation of amyloid from alpha-synuclein is dominated by reactions at hydrophobic interfaces. *Journal of the American Chemical Society, 132*(28), 9797–9803. https://doi.org/10.1021/ja102896h
- Sasso, L., Suei, S., Domigan, L., Healy, J., Nock, V., Williams, M. A. K., & Gerrard, J. A. (2014). Versatile multi-functionalization of protein nanofibrils for biosensor applications. *Nanoscale*, 6(3), 1629–1634. https://doi.org/10.1039/c3nr05752f
- Schrader, M., Pommerehne, K., Wolf, S., Finke, B., Schilde, C., Kampen, I., Lichtenegger, T., Krull, R., & Kwade, A. (2019). Design of a CFD-DEM-based method

- for mechanical stress calculation and its application to glass bead-enhanced cultivations of filamentous Lentzea aerocolonigenes. *Biochemical Engineering Journal*, 148, 116–130. https://doi.org/10.1016/j.bej.2019.04.014
- Serfert, Y., Lamprecht, C., Tan, C.-P., Keppler, J. K., Appel, E., Rossier-Miranda, F. J., Schroen, K., Boom, R. M., Gorb, S., Selhuber-Unkel, C., Drusch, S., & Schwarz, K. (2014). Characterisation and use of β-lactoglobulin fibrils for microencapsulation of lipophilic ingredients and oxidative stability thereof. *Journal of Food Engineering*, 143, 53–61. https://doi.org/10.1016/j.jfoodeng.2014.06.026
- Shezad, K., Zhang, K., Hussain, M., Dong, H., He, C., Gong, X., Xie, X., Zhu, J., & Shen, L. (2016). Surface roughness modulates diffusion and fibrillation of amyloid-β peptide. Langmuir: The ACS Journal of Surfaces and Colloids, 32(32), 8238–8244. https://doi. org/10.1021/acs.langmuir.6b01756
- Sluzky, V., Tamada, J. A., Klibanov, A. M., & Langer, R. (1991). Kinetics of insulin aggregation in aqueous solutions upon agitation in the presence of hydrophobic surfaces. *Proceedings of the National Academy of Sciences*, 88(21), 9377–9381. https:// doi.org/10.1073/pnas.88.21.9377
- Sukhanova, A., Poly, S., Bozrova, S., Lambert, É., Ewald, M., Karaulov, A., Molinari, M., & Nabiev, I. (2019). Nanoparticles with a specific size and surface charge promote disruption of the secondary structure and amyloid-like fibrillation of human insulin under physiological conditions. Frontiers of Chemistry, 7, 480. https://doi.org/ 10.3389/fchem.2019.00480
- Vargaftik, N. B., Volkov, B. N., & Voljak, L. D. (1983). International tables of the surface tension of water. *Journal of Physical and Chemical Reference Data*, 12(3), 817–820. https://doi.org/10.1063/1.555688
- Ye, X., Hedenqvist, M. S., Langton, M., & Lendel, C. (2018). On the role of peptide hydrolysis for fibrillation kinetics and amyloid fibril morphology. RSC Advances, 8 (13), 6915–6924. https://doi.org/10.1039/C7RA10981D
- Zarinwall, A., Waniek, T., Saadat, R., Braun, U., Sturm, H., & Garnweitner, G. (2021). Comprehensive characterization of APTES surface modifications of hydrous boehmite nanoparticles. *Langmuir: The ACS Journal of Surfaces and Colloids*, 37(1), 171–179. https://doi.org/10.1021/acs.langmuir.0c02682